Application of optimal design and control strategies to the forming of thin walled metallic components

Jean-Claude Gélin, Carl Labergere

Application of optimal design and control strategies to the forming of thin walled metallic components

J.C. Gélin, C. Labergere

Laboratoire Mécanique Appliquée R. Chaléat, UMR CNRS 6604, 24 rue de l'Epitaphe, 25030 Besançon, France

The paper focuses on approaches for the optimal process control in hydroforming. The main objective is to find by numerical simulation and optimisation the loading curve versus process parameters that minimise the thickness variations and that give the shape for the final part. Different approaches are proposed typically based on optimisation strategies and requiring a sensitivity analysis, or based on a local approximation of the tube thickness versus process parameters using optimisation procedures based on evolution strategies. The results obtained proved the ability of the proposed approach in the analysis of tube hydroforming processes and its potential to handle the numerical process control.

Keywords: Tube hydroforming; Finite element modelling; Sensitivity; Optimisation; Control of processes

1. Introduction

The use of FE simulations in sheet metal forming as well as in flanges or tubes produced by hydroforming processes is now strongly increasing in industry [2,7]. Such approaches are an economic way for virtual prototyping of parts and dies. The demand for extending the capabilities of actual FE software towards optimal process design and even control of processes is becoming very strong.

This paper focuses on the development and possibilities of optimisation [5] as well as control approaches in the simulation of sheet forming and flange/tube hydroforming processes. The developments are based both on optimisation methods and process control ones. The difficult problem concerning the formulation of the objective and constraint functions is first emphasised depending on the parameters to optimise. Then the paper deals with optimisation approaches where the gradients of the objective and constraint functions are evaluated from accurate sensitivity analyses. Different examples are provided illustrating the effectiveness of the proposed developments.

The second aspect concerns the control of processes where the problem consists of finding not only some process parameters but also how these parameters are evolving with time or with processing. This is the case when one tries to adjust the inner pressure versus axial feed in tube hydroforming [9]. In that case the optimisation techniques are not sufficient. An algorithm is proposed that first expresses the main driving variables as a function of the control ones by adjusting the local response to the control variables. Then the resulting objective functions for the control variables and constraint ones are determined step by step by optimisation. This process really permits control of the process variable versus processing time. Different cases have been already tested, such as the control of inner pressure versus axial feed in tube hydroforming in order to get the final part without defects and the results are fairly good.

2. Validation of the FEM solver

This validation example concerns the hydroforming of a T-shaped tube from a cylindrical one as it shown in Fig. 1. The initial outer diameter of the tube corresponds to 56.8 mm, whereas the initial tube thickness is 2.1 mm. The experimental investigations where carried on an aluminium alloy and the corresponding material properties are $E = 72{,}000$ MPa, $v = 0.32$, $\sigma_y = 40.74$ MPa and $\sigma_0 = 241(\varepsilon^{\text{eq}} + 0.00383)^{0.32}$ MPa.

The initial tube is put in the die cavity and axial symmetrical displacements are applied to both extremities of the tube. The required T-shape is reached under the inner pressure in Fig. 2. The simulation is carried out by imposing

* Corresponding author. Tel.: +33-3-81-66-60-35; fax: +33-3-81-66-67-00.
E-mail addresses: jean-claude.gelin@univ-fcomte.fr (J.C. Gelin), carl.labergere@univ-fcomte.fr (C. Labergere).

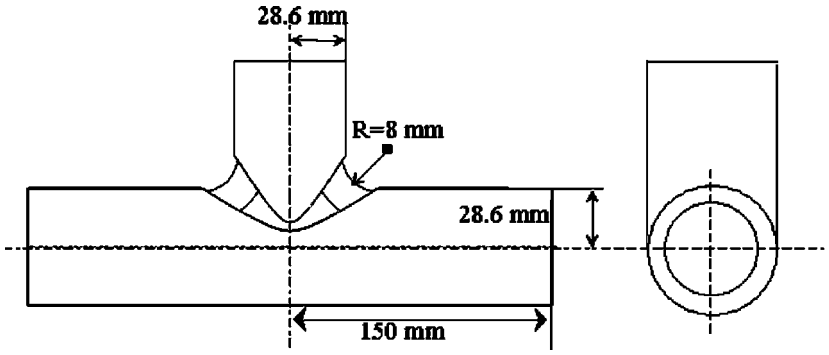

Fig. 1. Final geometry corresponding to the hydroforming of a T-shaped tube.

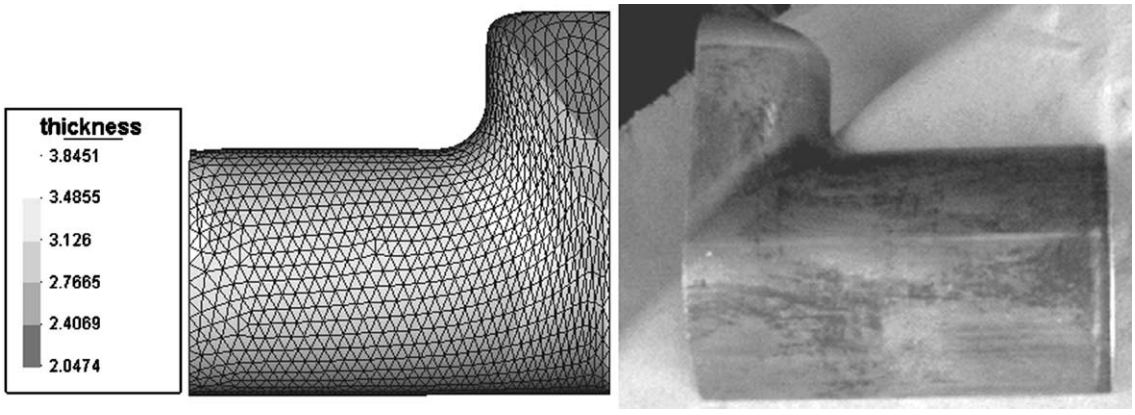

Fig. 2. A comparison between external shapes corresponding to the T-shaped tube obtained from experiment and from simulation.

both the axial displacements symmetrically to the tube extremities and the inner pressure. The deformed shapes corresponding both to experiment and simulation are compared in Fig. 2, that shows good agreement between simulation and experiment.

In order to accurately compare thicknesses obtained from experiments and from simulations, the lower and upper profiles of the T-shaped tube have been selected as indicated in Fig. 2. The thickness variation along both profiles are given in Fig. 3 and it can be noticed that the agreement between experiments and simulations is quite good even if the thickness variation amplitude is amplified along the lower profile and on the contrary decreased along the upper profile.

From the validation example, one can conclude that the ability of the direct solver is demonstrated for the simulation of tube hydroforming and that it can be used for the direct response calculations in the further developments.

3. Problem formulation

As extensively mentioned in the literature for tube hydroforming processes [1], the main problem in such processes is related to the adjustment of the loading path (inner pressure $p(t)$ versus axial feed $u(t)$) to get the component with the required shape and thickness. So the process parameters vector could be formulated as $\mathbf{q}(t) = \{p(t), u(t)\}$ and the optimal control problem for tube hydroforming expressed as follows. Find $p(t)$ the inner pressure and $u(t)$ the axial feed, so that the objective function with constraints are fulfilled:

$$\min_{\mathbf{q}(t)} f(p(t), u(t)) \quad \text{with} \quad g(p(t), u(t)) \leq \varepsilon_{\text{tol}} \tag{1}$$

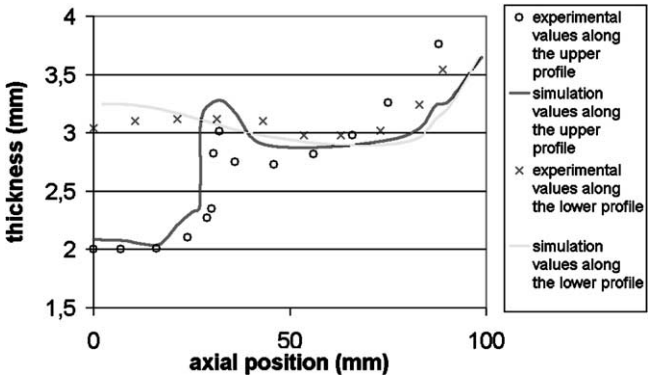

Fig. 3. A comparison of experimental and predicted thickness variation along upper profile and lower one for hydroforming of a T-shaped tube.

The objective function accounting for nodal thickness variation during the hydroforming process can be written as [3]

$$f(p(t),u(t)) = \left(\sum_{i=1}^{N} \left| \frac{h_i - h_0}{h_0} \right|^n \right)^{1/n}, \quad n = 1, 2 \text{ or } \infty \tag{2}$$

where N stands for the total number of nodes used for the simulation, h_0 the initial thickness, h_i the final thickness at node i and n is the power law parameter and is generally chosen to be 2, but it can be taken to 4 or 8 in some cases.

The constraint function $g(p(t),u(t))$ can be expressed in the following form:

$$g(p(t),u(t)) = 1 - \frac{\text{Vol}_{\text{num}}}{\text{Vol}_{\text{tube}}} \tag{3}$$

where Vol_{num} is the inner volume of the tube obtained from simulation, whereas Vol_{tube} is the inner volume desired. From this definition, it results that g measures the difference of required volume after hydroforming and the current one obtained by FEM simulations.

4. Optimisation

4.1. Sensitivity analysis

A methodology for sensitivity analysis of metal forming problems has been developed on the basis of direct differentiation of the solution procedure for the mechanical problem [5]. The increment of displacement Δu_{n+1} is obtained when the equilibrium is satisfied, following the explicit relationships:

$$a_{n+1} = \frac{F^{\text{ext}}_{n+1} - F^{\text{int}}_{n+1}}{m_{n+1}} \tag{4a}$$

$$v_{n+1} = v_n + a_{n+1}\,\Delta t_{n+1} \tag{4b}$$

$$\Delta u_{n+1} = V_{n+1}\,\Delta t_{n+1} \tag{4c}$$

The sensitivity of the displacement vector is obtained in the explicit case by solving the following equations:

$$\frac{\partial a_{n+1}}{\partial q_i} = \frac{(\partial F^{\text{ext}}_{n+1}/\partial q_i) - (\partial F^{\text{int}}_{n+1}/\partial q_i)}{m_{n+1}} - \frac{(F^{\text{ext}}_{n+1} - F^{\text{int}}_{n+1})(\partial m_{n+1}/\partial q_i)}{m^2_{n+1}} \tag{5a}$$

$$\frac{\partial v_{n+1}}{\partial q_i} = \frac{\partial v_n}{\partial q_i} + \frac{\partial a_{n+1}}{\partial q_i}\Delta t_{n+1} + a_{n+1}\frac{\partial \Delta t_{n+1}}{\partial q_i} \tag{5b}$$

$$\frac{\partial \Delta u_{n+1}}{\partial q_i} = \frac{\partial v_{n+1}}{\partial q_i}\Delta t_{n+1} + v_{n+1}\frac{\partial \Delta t_{n+1}}{\partial q_i} \tag{5c}$$

The sensitivity of the acceleration vector relative to the process parameter vector clearly depends on the internal load vector (5a) that is related to the sensitivity of the current stress tensor. So the following section describes the way to calculate this sensitivity. The yield criterion employed is the Hill quadratic one expressed as

$$f(\sigma, \bar{\varepsilon}^p_{n+1}) = \tfrac{1}{2}\boldsymbol{\sigma}\colon \mathbf{P} \colon \boldsymbol{\sigma} - \tfrac{1}{3}\sigma_0^2(\bar{\varepsilon}^p_{n+1}) \tag{6}$$

From Eq. (6), the increment of the plastic strain given by

$$\Delta \varepsilon^p = \Delta\lambda \frac{\partial f}{\partial \sigma} \tag{7}$$

where $\mathbf{P}$ is the orthotropic plastic tensor. The algorithm that is used corresponds to a predictor–corrector one when first an elastic stress state is calculated as $\boldsymbol{\sigma}^e_{n+1} = \mathbf{C}^e : \Delta\boldsymbol{\varepsilon}_{n+1}$, where $\mathbf{C}^e$ is the elasticity operator and $\Delta\boldsymbol{\varepsilon}_{n+1}$ is the strain increment. Then the plastic multiplier $\Delta\lambda$ is obtained from the plastic yield condition $f(\sigma, \varepsilon^p_{n+1}) = 0$. The sensitivity of the plastic multiplier using a direct differentiation method is given by

$$\begin{aligned}
&\frac{\partial \Delta\lambda}{\partial q_i} = \frac{G\Phi_1 - (2/3)\sigma_0(\bar{\varepsilon}^p_{n+1})\eta(\partial \bar{\varepsilon}^p_{n+1}/\partial p_i)}{G\Phi_2 + (4/9)\sigma_0^2(\bar{\varepsilon}^p_{n+1})\eta},\\
&\Phi_1 = \boldsymbol{\Phi}_3 : \left(\boldsymbol{\Pi} : \mathbf{C}^{e-1} \colon \frac{\partial \boldsymbol{\sigma}^e_{n+1}}{\partial q_i} \right),\\
&\Phi_2 = \boldsymbol{\Phi}_3 : (\boldsymbol{\Pi} : \mathbf{P} : \boldsymbol{\Pi} : \mathbf{C}^{e-1} \colon \boldsymbol{\sigma}^e_{n+1}),\\
&\boldsymbol{\Phi}_3 = (\mathbf{P} : \boldsymbol{\Pi} : \mathbf{C}^{e-1} \colon \boldsymbol{\sigma}^e_{n+1}), \;\; G = 1 - \frac{2}{3}\Delta\lambda\eta \text{ and } \Delta\lambda\eta,\\
&\boldsymbol{\Pi} = \left[\mathbf{C}^{e-1} + \Delta\lambda\mathbf{P}\right]^{-1} \sigma_0 = K(\bar{\varepsilon}^p_{n+1} + \varepsilon_0)^n \eta = nK(\bar{\varepsilon}^p_{n+1} + \varepsilon_0)^{n-1}
\end{aligned} \tag{8}$$

where σ_0 is given through a Swift hardening law.

This leads directly to the determination of the equivalent plastic strain sensitivity expressed as

$$\frac{\partial \bar{\varepsilon}^p_{n+1}}{\partial q_i} = \frac{(\partial \bar{\varepsilon}^p_n/\partial q_i) + (2/3)(\partial \Delta\lambda/\partial q_i)\sigma_0(\bar{\varepsilon}^p_{n+1})}{G} \tag{9}$$

Having the sensitivity of the effective plastic strain, one can then obtain the sensitivity of the stress tensor at each integration point expressed as

$$\begin{aligned}
&\frac{\partial \boldsymbol{\sigma}_{n+1}}{\partial q_i} = \boldsymbol{\Pi} : \mathbf{C}^{e-1} \colon \frac{\partial \boldsymbol{\sigma}^e_{n+1}}{\partial q_i} + \frac{\partial \boldsymbol{\Pi}}{\partial q_i} \colon \mathbf{C}^{e-1} \colon \boldsymbol{\sigma}^e_{n+1},\\
&\frac{\partial \boldsymbol{\Pi}}{\partial q_i} = -\frac{\partial \Delta\lambda}{\partial q_i}\boldsymbol{\Pi} : \mathbf{P} : \boldsymbol{\Pi}
\end{aligned} \tag{10}$$

4.2. Approximation of command laws for hydroforming

The adapted strategy consists of building an approximation for process parameters evolution laws versus time. This approximation could be formulated using a polynomial approximation or a more complex one depending on the complexity of the command law. To illustrate the proposed approach, one chooses a piecewise linear form for the pressure curve expressed as

$$p(t) = \frac{q_{i+1} - q_i}{t_{i+1} - t_i}t + \frac{q_i t_{i+1} - q_{i+1} t_i}{t_{i+1} - t_i} \tag{11}$$

where q_i are the process parameters and t is the normalised process time.

By differentiating such a function with respect to the parameter q_i, one get the following relationship:

$$\frac{\partial p(t)}{\partial q_i} = \frac{-t + (q_{i+1} - q_i)(\partial t/\partial q_i) + t_{i+1}}{t_{i+1} - t_i} \tag{12}$$

One can remark that the sensitivity vector clearly depends on the time step that has to be derived relatively to the process parameters vector.

4.3. A local optimisation method

In a first optimisation approach, one can choose an FSQP [6] method to solve the optimisation problem associated with Eq. (1). This method respects the constraints all along the optimisation path, avoiding non-realistic values for process parameters. The sensitivity analysis previously presented is used in this analysis.

The initial approximation of the pressure evolution law permits a definition of the initial conditions for the optimisation algorithm. If one takes $\{x^0\}$ as the vector for the initial interpolation parameters (q_i) used in Eq. (11), the optimisation algorithm generates a set of points $\{x^0\}, \{x^1\}, \ldots, \{x^k\}$ that normally converges to a local minimum of the objective function $f(p_s(t), u(t))$ defined by Eq. (2). At each iteration k, the next value is obtained from the previous one by

$$\{x^{k+1}\} = \{x^k\} + \alpha^k \{d^k\} \tag{13}$$

where $\{d^k\}$ is the descent direction and α^k is the scalar module in the direction $\{d^k\}$.

The optimisation algorithm determines the direction $\{d^k\}$ that permits a decrease in the objective function where α^k gives the module in that direction.

4.4. Application

The first application concerns the control for the problem corresponding to the expansion of a circular tube with a diameter equal to 40 mm and a thickness equal to 2 mm depicted in Fig. 4. Due to symmetry conditions, only one quarter of the problem is meshed with three nodes triangular shell elements. The material properties correspond to a mild carbon steel with $E = 2.1 \times 10^5$ MPa, $v = 0.3$, $\sigma_y =$ 250 MPa and $\sigma_0 = 551.44(\varepsilon^{eq} + 0.0621)^{0.284}$ MPa.

Fig. 5 relates the initial pressure versus axial feed curve before and after optimisation. One clearly see that the initial values are changed through the optimisation algorithm. In that example, the pressure and displacement are imposed for a normalised process time in the range 0–1, whereas the pressure and displacement values are unknown at the middle point $t = 0.5$.

In order to evaluate the sensitivity of the cost function and constraint one, the direct differentiation method (DDM) has been used and validated by performing comparisons with a standard finite difference method (FDM) that is easy to implement. The results concerning the sensitivity at the initial stage are given in Fig. 6 for the cost function and in Fig. 7 for the constraint function. It has to be noticed that DDM and FDM give similar results but it has also to be underlined that DDM is faster and generally more accurate than FDM.

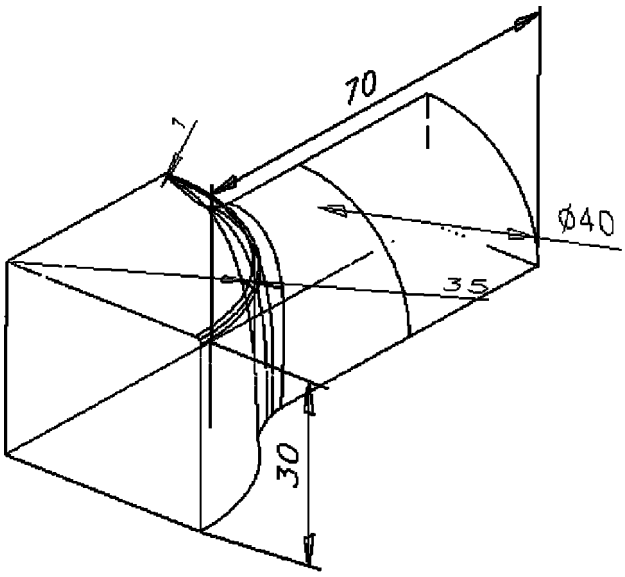

Fig. 4. Die geometry corresponding to the expansion of a circular tube.

During processing the sensitivity of the objective function varies with normalised process time and with process parameters. This is indicated in Fig. 8 where the zone in dark indicates that the constraint function is not satisfied. The values of process parameters corresponding to the optimisation path are also plotted in Fig. 8 and it clearly appears that the computation converges towards to a local minimum of the objective function.

Fig. 9 corresponds to the thickness contours after optimisation for the optimal process parameters.

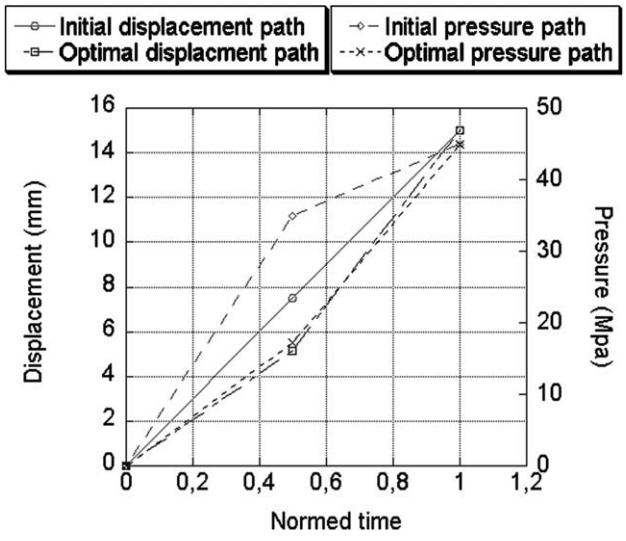

Fig. 5. Inner pressure vs. normalised time and axial feed vs. normalised time curves obtained from optimal control.

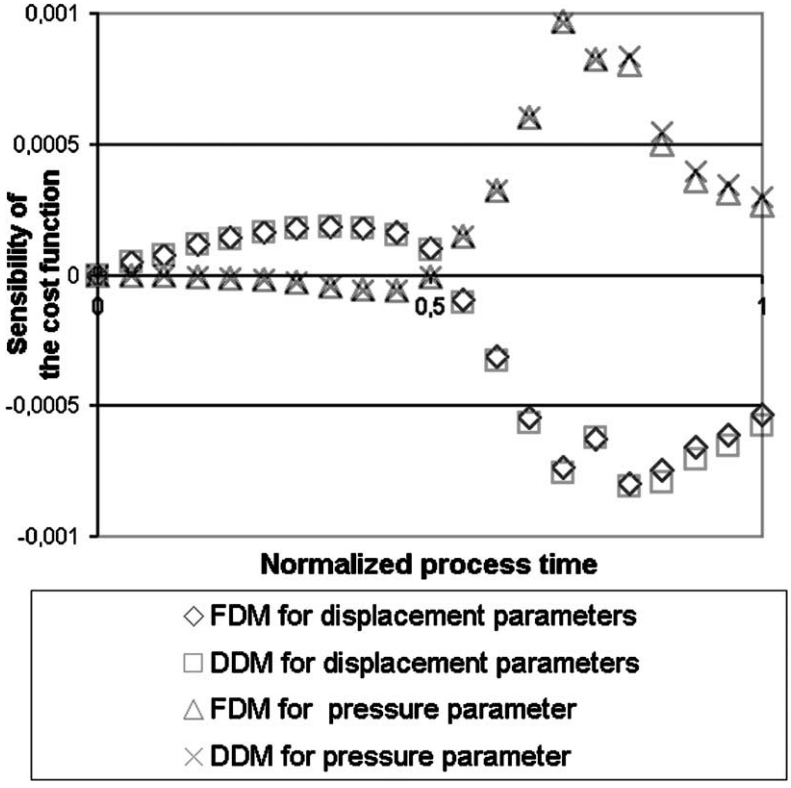

Fig. 6. Comparisons for the sensitivity of the cost function by DDM and FDM.

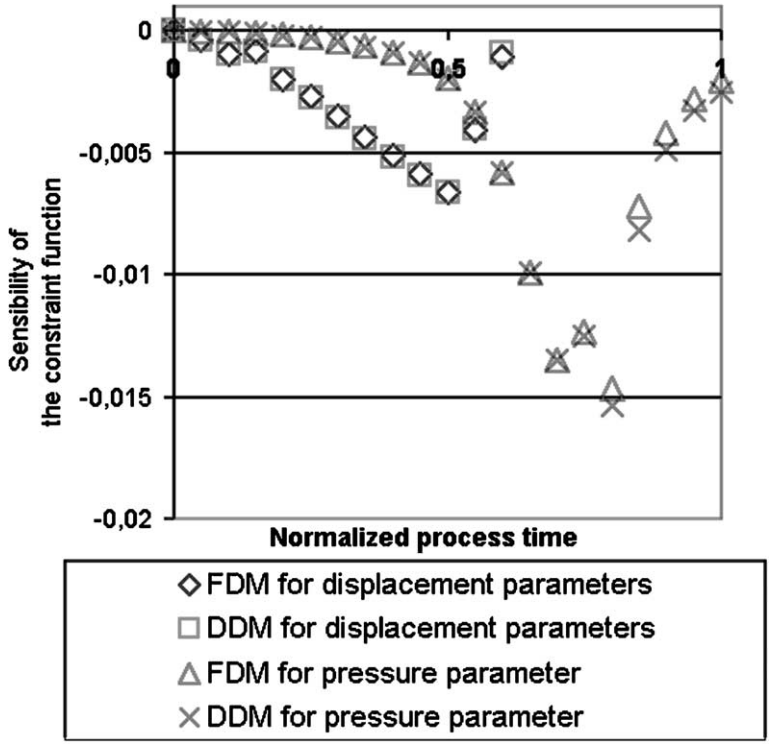

Fig. 7. Comparison of the sensitivity of the constraint function by DDM and FDM.

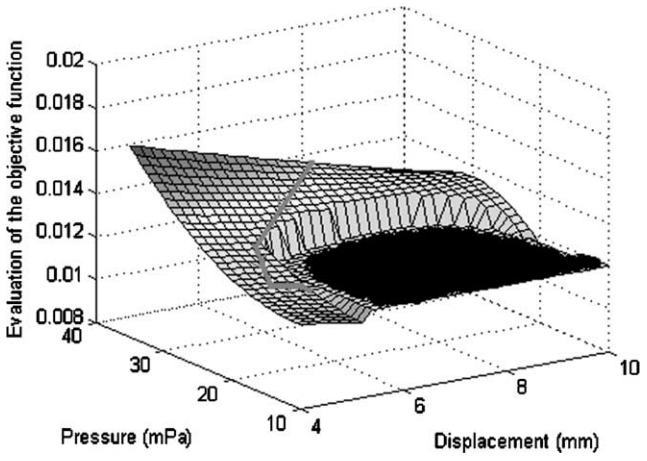

Fig. 8. Objective function vs. process parameters and optimisation path.

5. Optimal command procedure

5.1. The nodal thickness approximation

The procedure described in the previous section consists of a search of a set of process parameters describing the inner pressure versus axial feed curve in order to minimise the cost function expressed in terms of current tube thickness [4] over the domain under consideration. An alternative and a new way is proposed that consists of building an approximation of the current thickness (h) versus pressure (p) and axial feed (u), see Fig. 10.

A spline formulation is used for the interpolation of the local thickness versus pressure and axial feed u and it is expressed with coefficients $h^i_{\alpha\beta}$ that accounts for intermediate values from the minimal and maximal range for process parameters:

$$\begin{aligned} h(u,p) = {} & (1-\alpha)^2[(1-\beta)^2 h^i_{00} + a(1-\beta)\beta + \beta^2 h^i_{01}] \\ & + \alpha(1-\alpha)[b(1-\beta)^2 + c(1-\beta)\beta + d\beta^2] \\ & + \alpha^2[(1-\beta)^2 h^i_{10} + e(1-\beta)\beta + \beta^2 h^i_{11}] \end{aligned} \tag{14}$$

where α and β are determined from

$$\alpha = \frac{u-u_{\min}}{u_{\max}-u_{\min}} \quad \text{and} \quad \beta = \frac{p-p_{\min}}{p_{\max}-p_{\min}} \tag{15}$$

with $u_{\min} \le u \le u_{\max}$ and $p_{\min} \le p \le p_{\max}$.

In order to ensure continuity for the nodal approximation of thickness, the set of coefficients (a,b,c,d,e) are determined from the corners and midpoint values in the corresponding space to the Spline definition space $[0,1]\times[0,1]$:

$$\begin{aligned} & a = 4h^i_{0(1/2)} - h^i_{00} - h^i_{01}, \qquad b = 4h^i_{(1/2)0} - h^i_{00} - h^i_{10}, \\ & d = 4h^i_{(1/2)1} - h^i_{11} - h^i_{01}, \qquad e = 4h^i_{1(1/2)} - h^i_{11} - h^i_{10}, \\ & c = 16h^i_{(1/2)(1/2)} - (h^i_{00} + h^i_{01} + h^i_{10} + h^i_{11}) \\ & \qquad - (a+b+d+e) \end{aligned} \tag{16}$$

Then after the evaluation of the thickness at each node of the FE mesh, a genetic type optimisation algorithm [8] is used that provides the optimal process parameters. One can get the pressure versus axial feed optimal path from such an approach.

5.2. The constraint function

The constraint function has an important role to get the required shape of the part after processing as the aim of the process is to get the outer shape of the tubular component as defined by the inner shape of the die cavity at the end of the hydroforming stage. The optimisation method proposed above requires the use of a constraint function to satisfy such a condition that could be expressed as

$$\begin{aligned} & g^i(u,p) = \left| V^i_p - \frac{V^i_M - V^0_p}{N_{\text{eval}}} i - V^0_p \right| \le \varepsilon_{\text{tol}}, \\ & V^i_M = V^0_M - u \times \text{area} \end{aligned} \tag{17}$$

where the superscript i stands for ith optimisation step, V_p the outer tube volume, V_M the inner die cavity volume, N the number of necessary optimisation steps to reach the minimum and ε_{tol} is the fixed tolerance value. In using such a constraint function, one assumes that the outer volume increases during the simulation process.

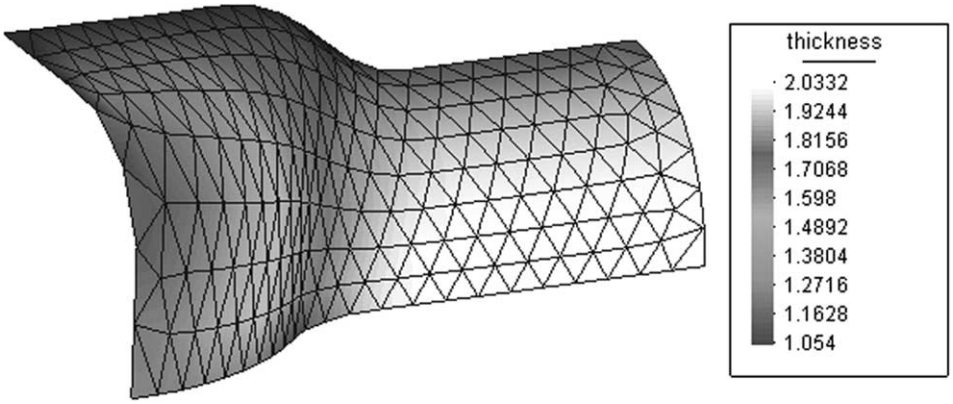

Fig. 9. Thickness contours corresponding to the optimal process path.

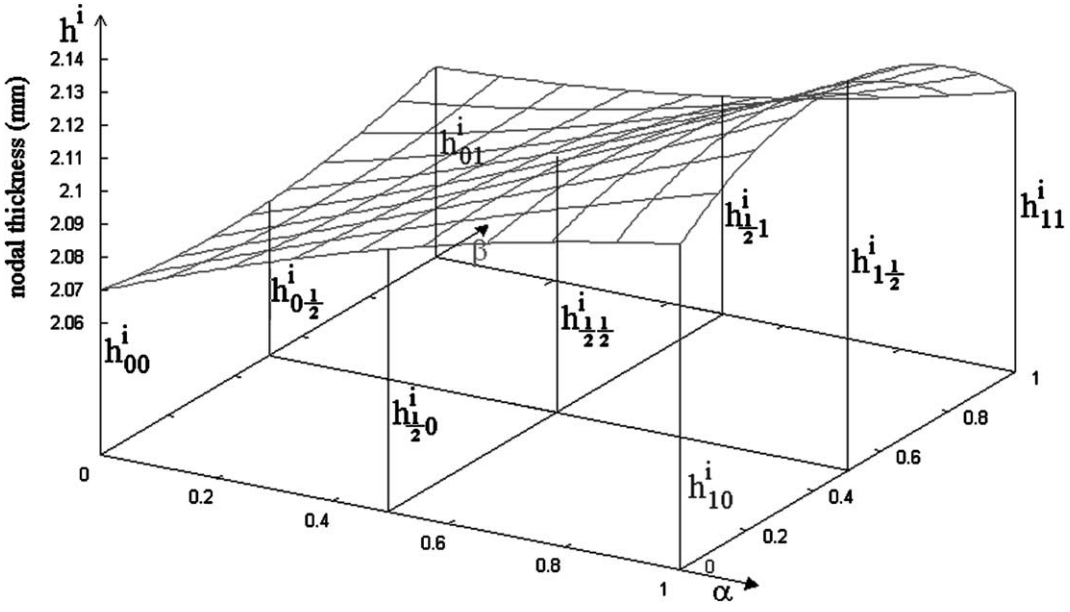

Fig. 10. Approximation of the nodal thickness h^i.

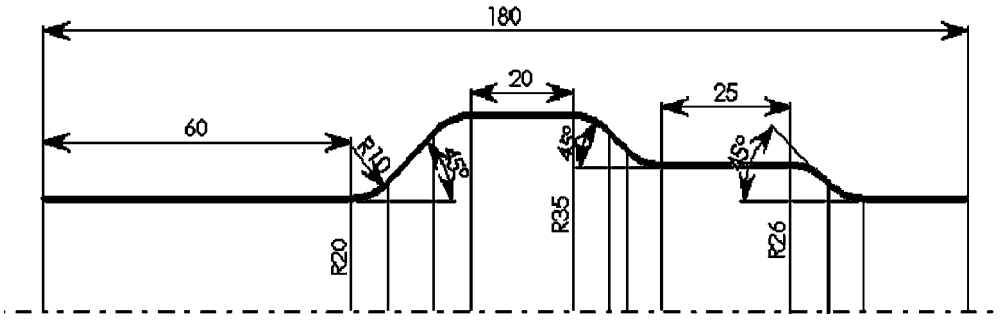

Fig. 11. Geometry of the die cavity and tubular shape for the multistage radial expansion of a cylindrical tube.

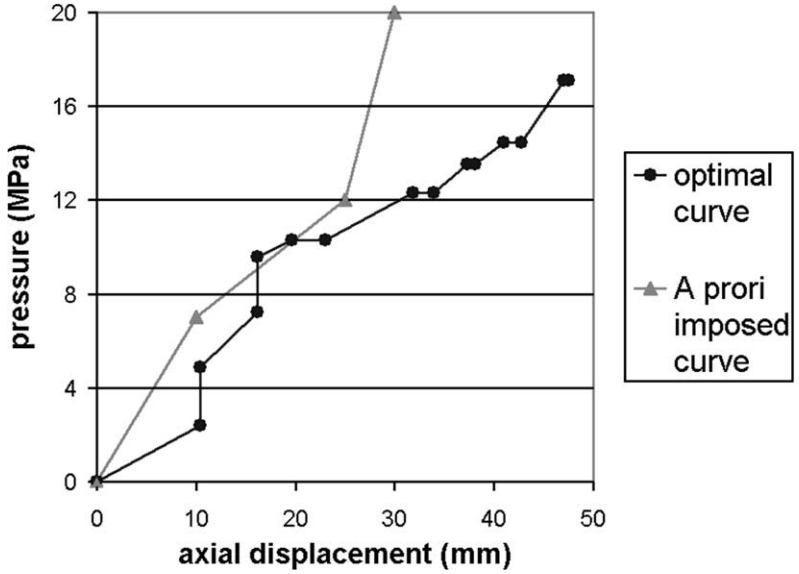

Fig. 12. Inner pressure vs. axial feed curve obtained from optimal control of the multistage radial expansion of a cylindrical tube.

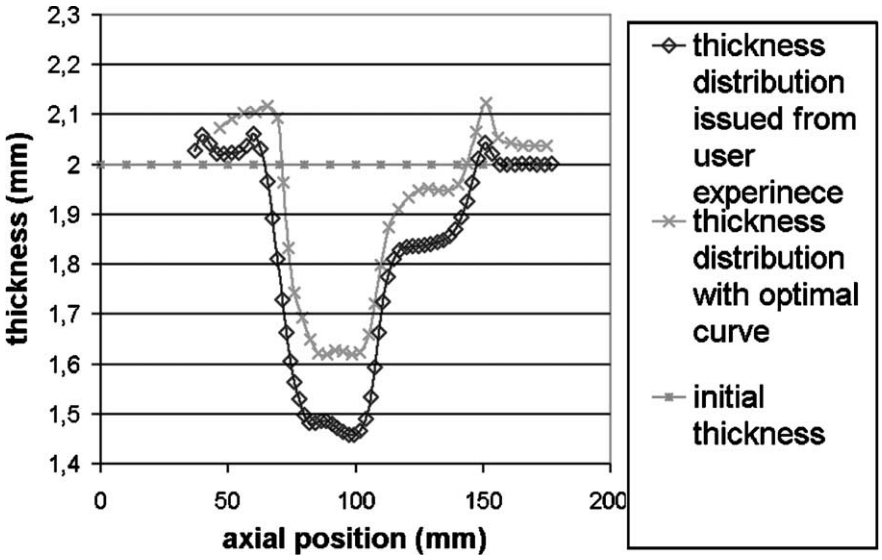

Fig. 13. Thickness variation along the tube axis for the optimal inner pressure vs. axial feed loading path in comparison with an a priori fixed loading path.

5.3. Multistage radial expansion of a cylindrical tube

The proposed example is associated with the optimisation and control problem related to the radial expansion of a circular cross section tube with an initial inner diameter equal to 60 mm and an initial thickness equal to 2.1 mm, the geometry of the final part is given in Fig. 11 and the material properties are: $E = 72{,}000$ MPa, $\nu = 0.32$, $\sigma_y = 40.74$ MPa and $\sigma_0 = 241(\varepsilon^{\text{eq}} + 0.00383)^{0.32}$ MPa.

In that example, one searches to get the optimal pressure versus axial feed optimal curve. The optimisation is a step by step one that leads to the optimal control path related in Fig. 12.

The thickness variation along the tube axis corresponding to optimal inner pressure versus axial feed path is reported in Fig. 13 in comparison with an a priori determined loading curve issued from an a priori set of parameters issued from user experience.

It is demonstrated that the use of the proposed control procedure really leads to decreased thickness variation during processing.

6. Conclusions

Two distinct procedures have been proposed for the optimisation and control of the hydroforming process. The first one is directly related to optimisation in the sense that the control is defined in terms of process parameters and these parameters serve as optimisation ones. A sensitivity analysis is required to apply a gradient-based optimisation method and the optimisation of the control curve is then realised. This procedure gives accurate results as described in the paper but necessitates numerous computations. The second strategy is a step by step one that consists of an approximation to the main quantity entering in the cost function (thickness) versus process parameters and then to get at the end of the process the control curve. It has been shown that this approach gives accurate results and corresponds well to the requirements associated with process control in hydroforming. The results obtained are very encouraging and show that numerical control can help the process designers.

References

[1] T. Altan, M. Koç, Y. Aue-u-lan, K. Tibari, Formability and design issues in tube hydroforming, in: Proceedings of the First International Conference on Hydroforming, 1999, pp. 105–121.

[2] J.C. Gelin, P. Picart (Eds.), Proceedings of the Fourth International Conference and Workshop on Numerical Simulation of 3D Sheet Forming Processes, Burs Publishers Besanson-France, 1999.

[3] J.C. Gelin, O. Ghouati, C. Labergere, From optimal design to control of process in hydroforming of tubes, in: Proceedings of the Seventh International Conference on Numerical Methods for industrial Forming Processes, 1999.

[4] J.C. Gelin, C. Labergere, Numerical design and optimal control of sheet forming and tube hydroforming processes, in: E. Ouate (Ed.), Proceedings of the NUMIFORM 2001 Conference, 2001, CD-ROM Publications.

[5] O. Ghouati, H. Lenoir, J.C. Gelin, Optimal design of forming processes using the finite element method, Adv. Eng. Mater. 2/7 (2000) 438–442.

[6] C. Laurence, J.L. Zhou, A.L. Tits, User's Guide for CFSQP, Version 2.5, Internal report, University of Maryland, College Park-USA, 1997, http://www.isr.umd.edu/Labs/CARSE/FSQP/efsa.p-manual.pdf.

[7] K.I. Mori (Ed.), Simulation of materials processing: theory, methods and application, in: Proceedings of the Seventh International Conference on Numerical Methods in Industrial Forming (NUMIFORM 2001), A.A. Balkema Publishers Toyko-Japan, 2001.

[8] Z. Michalewicz, G. Nazhiyath, Genocop III: a co-evolutionary algorithm for numerical optimization problems with nonlinear constraints, in: Proceedings of the Second IEEE International Conference on Evolutionary Computation, Vol. 2, Perth, 1995, pp. 647–651.

[9] M. Strano, S. Jirathearanat, T. Altan, Adaptive FEM simulation for tube hydroforming: a geometry based approach for wrinkle detection, Ann. CIRP 50/1 (2001) 185–190.